J. Biochem. **138**, 89–94 (2005)
DOI: 10.1093/jb/mvi102

Expression in *Escherichia coli*, Purification and Characterization of *Thermoanaerobacter tengcongensis* Ribosome Recycling Factor

Peng Guo[1], Liqiang Zhang[1], Zhen Qi[2], Runsheng Chen[2] and Guozhong Jing[1,*]

[1]National Laboratory of Biomacromolecules and [2]Molecular Biology Center, Institute of Biophysics, Chinese Academy of Sciences, Beijing 100101, P.R. China

Received March 16, 2005; accepted May 1, 2005

A very promising approach to understanding the mechanism of protein thermostability is to investigate the structure–function relationship of homologous proteins with different thermostabilities. Ribosome recycling factor (RRF), which is an essential factor for protein synthesis in bacteria, may be a good candidate for such study. In this report, a ribosome recycling factor from *Thermoanaerobacter tengcongensis* was expressed and characterized. This protein contains 184 residues, shows 51.4% identity to that of *Escherichia coli* RRF, and has very strong antigenic cross-reactivity with antibody to *E. coli* RRF. *In vivo* activity assay shows that weak residual activity may remain in *Tte*RRF in *E. coli* cells. Circular dichroism spectral analysis shows that *Tte*RRF has a very similar secondary structure to that of *E. coli* RRF, implying that they have similar tertiary structures. However, their thermostabilities are significantly different. To find which domain of RRF is mainly responsible for maintaining stability, *Tte*DI/*Eco*DII and *Eco*DI/*Tte*DII RRF chimeras were created. Their domain I and domain II are from *E. coli* and *T. tengcongensis* RRFs, respectively. The results of GdnHCl and heat induced denaturation of the chimeric RRFs suggest that the domain I plays a major role in maintaining the stability of the RRF molecule.

Key words: expression and characterization, ribosome recycling factor, *Thermoanaerobacter tengcongensis*, thermostability.

The molecular basis of the thermal stability of globular proteins is a highly significant yet unsolved problem. In recent years, considerable effort has been made to understand the mechanisms that determine the thermal stability of proteins using various approaches (*1*). A very promising approach is the investigation of the structure–function relationship of homologous proteins from mesophilic and thermophilic sources. Ribosome recycling factor (RRF) is an essential factor for protein synthesis in bacteria and in eukaryotic organelles (*2*, *3*), and is required for the disassembly of the post-termination complex, freeing the ribosome for the next round of translation (*2*, *4–7*). To date, all reported RRFs are highly homologous in amino acid sequence (*8*, *9*), and several crystal structures of RRFs from thermophilic (*8*, *10*) and mesophilic (*11–13*) bacteria have been determined. All of these structures are similar and consist of two domains: domain I displays a three-helix bundle structure, and domain II exists as a three layer β/α/β sandwich structure. However, there is a significant difference in the thermostabilities of the RRFs from thermophilic and mesophilic bacteria. The unique features make RRF proteins a good model for studies of the mechanism of protein thermostability. As a first step, it is very interesting to know whether the two domains make the same contribution to maintaining the stability of the RRF molecules, and if they do not, which domain plays a major role. To answer these questions, a ribosome recycling factor from *Thermoanaerobacter tengcongensis* was first expressed in *Escherichia coli* cells and characterized. Then, two RRF chimeras, *Eco*DI/*Tte*DII and *Tte*DI/*Eco*DII, were created. *Eco*DI/*Tte*DII consists of domain I from *E. coli* and domain II from *T. tengcongensis* RRF. *Tte*DI/*Eco*DII consists of domain I from *T. tengcongensis* and domain II from *E. coli* RRF. To test the changes in stability of the chimeric RRFs, and to find which domain plays a major role in maintaining the stability of the RRF molecules, GdnHCl and heat induced denaturation of the RRFs was measured by monitoring changes in the circular dichroism (CD) signal at 222 nm. The results show that the *T. tengcongensis* RRF protein contains 184 residues, and is very closely related to *Escherichia coli* RRF in sequence and structure; however, there is a significant difference in thermostability between them. The results of GdnHCl and heat induced denaturation of the chimeric RRFs suggest that domain I is mainly responsible for the stability of the RRF molecule. This information will be helpful for further studies of the molecular mechanism of the protein thermostability.

MATERIALS AND METHODS

Bacterial Strains, Plasmids, and Culture Conditions—*Thermoanaerobacter tengcongensis* MB4 is a rod-shaped, gram-negative bacterium that propagates optimally at 75°C. It was isolated recently from a hot spring in Tengcong, China (*14*). It was used to prepare the genomic DNA for amplifying the *T. tengcongensis* RRF gene (*frr*) in this study. *E. coli* LJ14 is a MC1061 strain (frr^{ts}), of which the chromosomal wild-type *frr* allele is replaced

*To whom correspondence should be addressed. Tel: +86-10-64879271, Fax: +86-10-64840672, E-mail: jinggzh@sun5.ibp.ac.cn

with a mutant allele (Val117Asp) (*15*), allowing *E. coli* LJ14 to grow at 30°C but not at 42°C. For analysis of the complementation of *E. coli* LJ14 (*frr*^{ts}), *E. coli* LJ14 harboring various plasmid constructs was grown overnight at the permissive temperature (30°C). Cultures in LB medium containing ampicillin (60 μg/ml) and IPTG (0.4 mM) were started with a 0.06% (v/v) inoculum from freshly grown (at 30°C) overnight cultures, and the growth at both the permissive (30°C) and non-permissive (42°C) temperatures was monitored by recording culture turbidities at 600 nm at regular intervals. pET-DB was constructed in our laboratory (*16*) and used for the expression of *T. tengcongensis* RRF (*Tte*RRF) in this study. Besides the common control elements found in the pET system, there is an important translation signal, the downstream box (DB) downstream of the initiation codon in the vector that can enhance protein expression in *E. coli* (*16*, *17*). pQE-60 is a vector with a strong T_5 promoter purchased from QIAGEN. It was used to construct pQE-*Tte*RRF and pQE-*Eco*RRF for analysis of the complememtation of *E. coli* LJ14 (*frr*^{ts}).

Cloning of RRF Genes (frr) from T. tengcongensis and E. coli—Based on the putative RRF gene sequence of *T. tengcongensis* (*14*), forward (5′-GGT ACC ATG GGT AGC GAT TAT TTG AAA GAC AGT G-3′) and reverse (5′-GAT TGG ATC CTT AAA TTT CCA TTA TCT CCT TTT C-3′) primers containing *Nco*I and *Bam*HI restriction sites, respectively, were designed to amplify the open reading frame (ORF) corresponding to RRF by PCR using genomic DNA from *T. tengcongensis* MB4 as a template DNA. PCR was performed using *pfu* DNA polymerase (New England Biolabs); the cycling conditions included an initial template denaturation step at 94°C for 5 min followed by 30 cycles of incubations at 94°C for 0.5 min, 55°C for 0.5 min and 72°C for 1 min. After extension at 72°C for 7 min, the PCR product of the expected size was obtained, digested with *Nco*I and *Bam*HI, and cloned into the same sites of pET-DB (*16*), resulting in pET-DB-*Tte*RRF for the expression of *Tte*RRF. The authenticity of the cloned *Tte*RRF gene was verified by DNA sequence analysis. Subsequently, the RRF gene was also cloned into the pQE-60 vector between the *Nco*I and *Bam*HI restriction sites, resulting in pQE-*Tte*RRF for the analysis of complementation.

For cloning of the RRF gene from *E. coli*, forward (5′-GGC ACC ATG GGT ATT AGC GAT ATC AGA AAA GAT GC-3′) and reverse (5′-GCT GCT CGA GGA ACT GCA TCA GTT CTG CTT CTT TG-3′) primers containing *Nco*I and *Xho*I restriction sites, respectively, were used to amplify the *E. coli* RRF gene from *E. coli* genomic DNA. The reaction conditions were the same as detailed for the amplification of the *Tte*RRF gene. The PCR product was digested with *Nco*I and *Xho*I and cloned into pET-28a(+) after digestion with the same enzymes, resulting in pET28-*Eco*RRF. This expression vector was used for the expression of *Eco*RRF. The *Eco*RRF gene was also cloned into the pQE-60 vector between the *Nco*I and *Bam*HI sites, resulting in pQE-*Eco*RRF, which was used for the complementation assay.

Cloning of Chimeric RRF Variants—Two chimeric RRF variants were constructed using gene SOEing (*18*). For construction of the *Eco*DI/*Tte*DII chimera gene, six primers were designed. Primers 1 and 2 were the same as the forward and reverse primers for cloning the RRF gene from *E. coli* as described above. The other four primers were as follows: primer 3 (5′-AGG GCC GGA TTC GCT CTA CCC GTG CGT ATT TTG CTG-3′), primer 4 (5′-CAG CAA AAT ACG CAC GGG TAG AGC GAA TCC GGC CCT-3′), primer 5 (5′-GTT CTT CCG TCA GCG GTG GAA GGA CCA GTC TTA G-3′), primer 6 (5′-CTA AGA CTG GTC CTT CCA CCG CTG ACG GAA GAA C-3′). Each primer contains a priming sequence for the amplification of the *Eco*RRF gene or the *Tte*RRF gene and also has an overlap sequence at its 5′ end (bold) that is complementary to a segment of the *Eco*RRF gene or the *Tte*RRF gene. Five polymerase chain reactions were performed using the pQE-*Eco*RRF or pQE-*Tte*RRF plasmid as a template. The PCR product was digested with *Nco*I and *Xho*I and cloned into pET-28a(+) after digestion with the same enzymes, resulting in pET28-*Eco*DI/*Tte*DII. This expression vector was used for the expression of *Eco*DI/*Tte*DII. The *Tte*DI/*Eco*DII chimera gene was created by using the same strategy, resulting in pET28-*Tte*DI/*Eco*DII for the expression of *Tte*DI/*Eco*DII.

Expression and Purification of TteRRF, EcoRRF, and Chimeric RRF Variants—Each plasmid was transformed into *E. coli* BL21(DE3)pLysS cells. Transformants were grown in LB medium supplemented with 50 μg/ml kanamycin and 25 μg/ml chloramphenicol overnight at 37°C for small scale culture. The overnight culture (20 ml) was then diluted 50-fold with the same medium, and incubated at 37°C until a turbidity of 0.6–0.8 at 600 nm was obtained prior to induction by 0.4 mM IPTG for 4 h. The cell pellet was collected by centrifugation at 6,000 × *g* for 20 min at 4°C, re-suspended in 45 ml of chelating buffer (25 mM Tris-HCl, pH 8.0, 500 mM NaCl, and 10 mM imidazole), and frozen at –20°C until later use.

Because twenty-two amino acid residues including a His_6-tag and a thrombin cleavage site were fused in-frame to the N-terminal end of *Tte*RRF when the *Tte*RRF gene was cloned into pET-DB vector (*16*), the *Tte*RRF protein was first expressed as a His_6-tagged protein. To purify the His_6-tagged *Tte*RRF protein, the above bacterial cells were thawed at 37°C, ultrasonicated on ice for 1 min × 5 to break the cells, and then the supernatant (40 ml) was recovered after the lysed bacteria were centrifuged at 37,000 × *g* at 4°C for 30 min. The supernatant was applied directly onto a 5 × 1 cm^2 of chelating Sepharose Fast Flow column at a flow rate 1.0 ml/min, which was charged with Ni^{2+} prepared according to the producer's protocol (Amershan Pharmacia Biotech) and equilibrated with the chelating buffer. The column was washed first with 50 ml of chelating buffer followed by 50 ml of washing buffer (25 mM Tris-HCl, pH 8.0, 500 mM NaCl, 80 mM imidazole). Finally, the column was eluted with elution buffer (25 mM Tris-HCl, pH 8.0, 500 mM NaCl, 200 mM imidazole), and monitored by absorbance at 280 nm. The major peak of protein was collected and then dialysed against distilled water at 4°C. The protein was lyophilized and stored at –20°C. The purified fusion protein was then incubated with thrombin (Sigma T4648) in the ratio of 10 units of thrombin mg^{-1} protein in cleavage buffer (20 mM Tris-HCl, pH 8.0, 2.5 mM $CaCl_2$, 10 mM $MgCl_2$) at 4°C for 8 h. After digestion, the cleavage mixture was applied onto the second metal chelating chromatography column to remove the fusion partner.

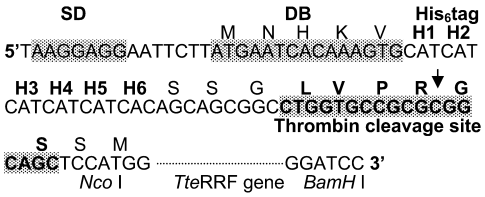

Fig. 1. **The relative position of the ribosome binding site (SD), the downstream box (DB) downstream of the initiation codon, and the His_6-tag and thrombin cleavage site coding sequences in the expression vector pET-DB-*Tte*RRF.** Arrow indicates the thrombin cleavage site.

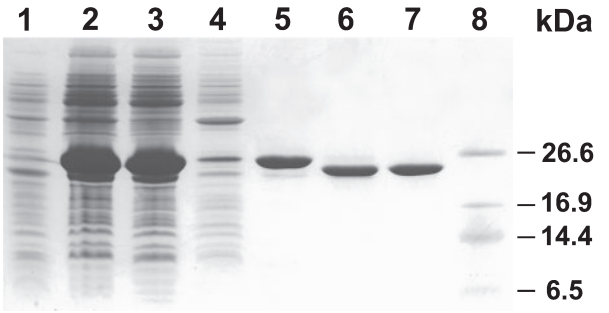

Fig. 2. **SDS–15%PAGE analysis of the expression and purification of the *Tte*RRF protein.** The gel was stained with Coomassie Brilliant Blue R250. Lane 1: total protein extract before IPTG induction. Lane 2: total protein extract after IPTG induction for 4 h. Lane 3: supernatant of the induced cell after lysis. Lane 4: precipitate of the induced cell after lysis. Lane 5: major peak of the first chelating affinity chromatography. Lane 6: mixture after thrombin cleavage. Lane 7: major peak from the second chelating affinity chromatography. Lane 8: molecular mass markers (BioRad).

*Eco*RRF, and Chimeric RRF Variants were purified using the same methods as described above.

The protein samples at each step were analyzed by SDS–15% polyacrylamide gel electrophoresis (SDS-PAGE) according to the Blackshear procedure (*19*). Protein concentrations were determined according to the method described (*20*).

Mass Spectrographic Analysis—For mass measurement, a protein sample (10 pmol) was dissolved in 40 μl of a solution containing 50% acetonitrile and 0.1% trifluoroacetic acid for MALDI-TOF-MS analysis. A freshly prepared solution of α-cyano-4-hydroxycinnamic acid (10 mg/ml) in 70% acetonitrile and 0.1% trifluoroacetic acid was mixed with the same volume of the above sample solution. A total of 1.0 μl of sample mixture was applied to the MALDI target and allowed to dry. A MALDI-TOF mass spectrum was acquired on an AXIMA-CFP plus mass spectrometer equipped with a 337.1-nm nitrogen laser. Data from 100 laser shots were averaged for each spectrum.

Western Blotting Analysis—Polyclonal antibodies against *E. coli* RRF were raised in New Zealand rabbits by the standard method (*21*) using Freund's incomplete adjuvant. Immunoblot horseradish peroxidase (HRP) assays (*22*) were used to analyze antigenic cross-reactivity of *Tte*RRF with the antibody against *E. coli* RRF in this study.

Circular Dichroism Spectra and GdnHCl and Heat Induced Denaturation of RRFs—Circular dichroism (CD) spectra were recorded at 25°C using an Applied Photophysics PiStar-180 spectrometer with a 1 mm pathlength quartz cuvette. The protein concentration in the samples was 0.1 mg/ml for far-UV CD (250–200 nm) in 50 mM sodium phosphate buffer, pH 7.4. The CD spectral data represent the average of four scans after correction for the buffer baseline and are reported as mean residue ellipticity ([θ]).

Guanidine hydrochloride (GdnHCl) and heat induced denaturation of RRFs was measured by monitoring the changes in the circular dichroism (CD) signal at 222 nm. For GdnHCl induced denaturation, proteins were incubated with the required concentration of GdnHCl at 25°C overnight to allow the samples to reach equilibrium as indicated by no further CD change. For heat induced denaturation, proteins were heated at 1°C per minute from 25°C to 85°C using the PC.2 Peltier temperature controller accessory of the PiStar-180 instrument. The cuvette was sealed with parafilm to prevent evaporation while the pressure was kept relatively constant.

RESULTS AND DISCUSSION

Construction of the TteRRF Expression Plasmid—As described in "MATERIALS AND METHODS," the *Tte*RRF coding sequence was synthesized by PCR and cloned into vector pET-DB (*16*), resulting in pET-DB-*Tte*RRF for the expression of the *Tte*RRF gene. Figure 1 shows the relative positions of the SD sequence, DB sequence, and the His_6-tag and thrombin cleavage site coding sequences in the expression vector. The oligonucleotide sequence, which encodes 22 amino acid residues including His_6-tag and thrombin cleavage site coding sequences, was fused in-frame to the coding sequence of the *Tte*RRF protein at the *Nco*I restriction endonuclease site. In this case, the *Tte*RRF gene was first expressed as a His_6-tagged fusion protein. Moreover, the His_6-tag and specific protease thrombin cleavage sequences simplify purification of the *Tte*RRF protein.

Table 1. **Purification summary.**

Purification step	Volume (ml)	Total protein (mg)	Yield (%)
Supernatant of cell lysate	40	ND	ND
Ni^{2+} chelating affinity chromatography	20	80	100
The second Ni^{2+} chelating affinity chromatography	25	50	62.5

The data were obtained in the purification of *Tte*RRF protein from 1 liter of bacterial culture as described in "MATERIALS AND METHODS." The *Tte*RRF protein was first expressed and purified as a His_6-tagged protein. About 50 mg of homogeneous *Tte*RRF protein was finally obtained by passage through a second metal chelating chromatography column after cleavage of the purified His_6-tagged *Tte*RRF sample with thrombin.

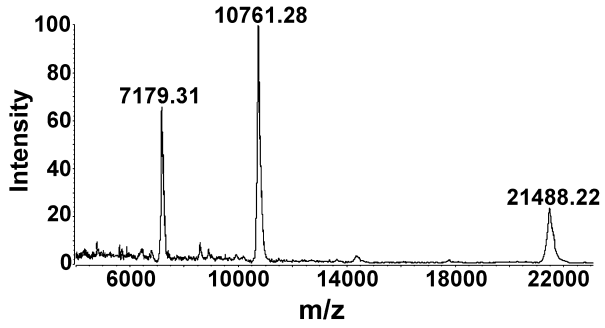

Fig. 3. **MALDI-TOF mass spectrum of *Tte*RRF.** The sample (10 pmol) was dissolved in 50% acetonitrile and 0.1% (v/v) TFA and applied onto the target. α-Cyano-4-hydroxycinnamic acid (CCA) was used as the matrix. The range was set as 4,000–24,000 Da.

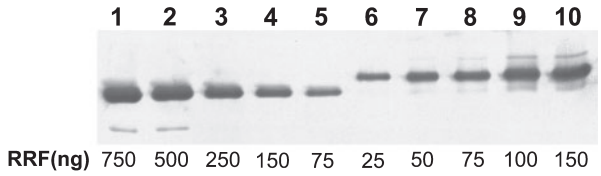

Fig. 4. **Antigenic cross-reactivity of *Tte*RRF with an antibody against *E. coli* RRF.** The purified RRF was separated by SDS-PAGE. The protein samples were then transferred onto a nitrocellulose membrane and hybridized with 1:2,000 diluted rabbit antibody against *Eco*RRF. The immunoblot horseradish peroxidase (HRP) assay system was used to develop the membrane. Lanes 1 to 5 contain 750, 500, 250, 150, 75 ng of *Tte*RRF, respectively. Lanes 6 to 10 contain 25, 50, 75, 100, 150 ng of *Eco*RRF, respectively.

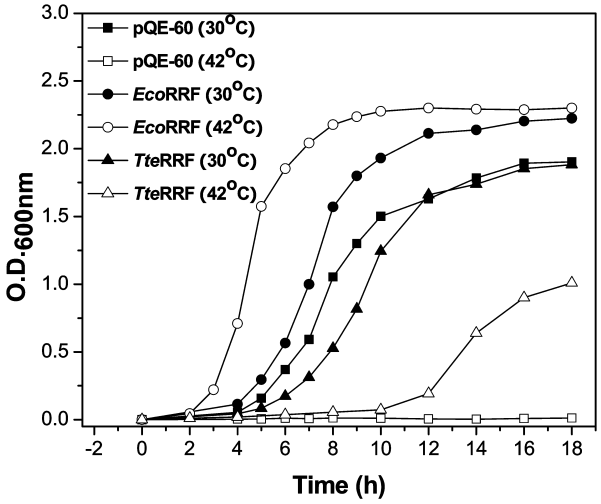

Fig. 5. **Analysis of complementation of *E. coli* LJ14 (*frr*^{ts}) with *T.tengcongensis* RRF.** Growth of *E. coli* LJ14 (*frr*^{ts}) transformants at the permissive (30°C, filled symbols) and non-permissive (42°C, open symbols) temperatures as described in the text. The growth of the cultures ($OD_{600\ nm}$) was monitored at regular intervals. The transformants harboring either vector alone (pQE-60) or pQE-*Tte*RRF and pQE-*Eco*RRF expressing *Tte*RRF and *Eco*RRF, respectively, as indicated in the inset.

Soluble Expression of the His$_6$-Tagged TteRRF Protein—Expression of the His$_6$-tagged *Tte*RRF gene in *E. coli* was analyzed by SDS-PAGE. Figure 2 shows the 15% SDS-PAGE pattern of the cell lysate from *E. coli* cells harboring pET-DB-*Tte*RRF before and after induction with IPTG for 4 h. A very intensely staining protein band can be observed in the induced total cell lysate (Fig. 2, lane 2), but not in the uninduced cell lysate (Fig. 2, lane 1). It is noteworthy that the PAGE pattern of *Tte*RRF in the supernatant sample (Fig. 2, lane 3) is almost the same as that in the induced total cell extract. The results indicate that the desired recombinant RRF protein is highly expressed in a soluble form accounting for more than 39% of the total cellular proteins of the bacterial cell as indicated by scanning the protein density of the gel.

Purification and Characterization of the TteRRF Protein—The purification procedure based on 1 liter of culture is summarized in Table 1. His$_6$-tagged *Tte*RRF was first purified to apparent homogeneity in one step by Ni^{2+}

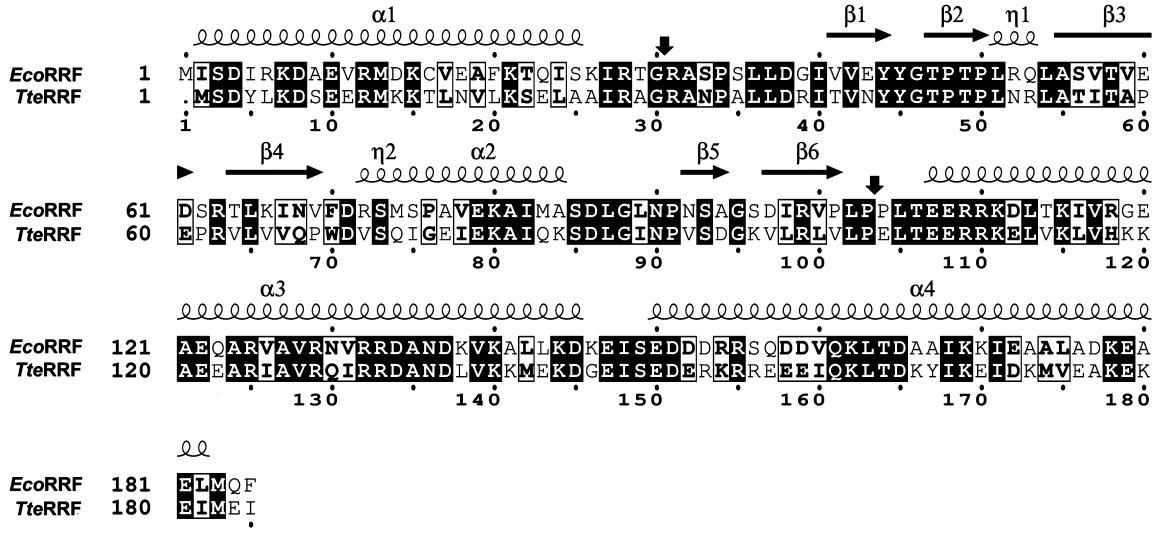

Fig. 6. **Comparison of the primary structures of *Eco*RRF and *Tte*RRF.** Amino acids are shown as single letter codes. The numbering at the bottom is according to the sequence of *E. coli* RRF. Identical residues are shadowed in black and similar residues are boxed. The secondary structure elements of *Eco*RRF are shown at the top. The two vertical arrows indicate the points where the two domains were exchanged (G30 and R31, P103 and P104 for *Eco*RRF; G29 and R30, P102 and E103 for *Tte*RRF, respectively).

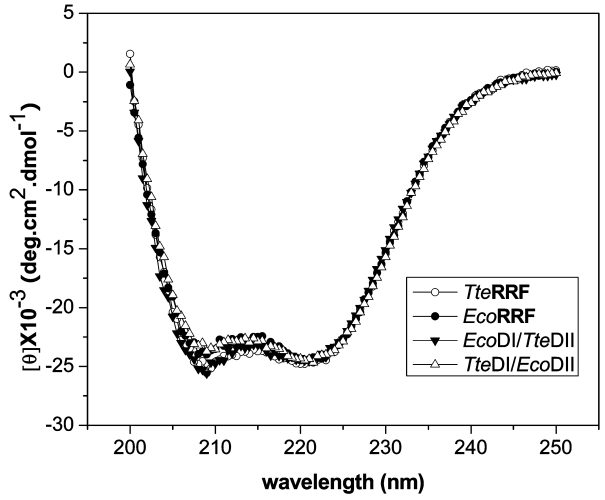

Fig. 7. **Far-UV CD spectra of *Tte*RRF, *Eco*RRF, and their chimeras.** Proteins were dissolved in 50 mM sodium phosphate buffer, pH 7.4, at a concentration of 0.1 mg/ml. The analysis was carried out at 25°C, and the data are reported as mean residue ellipticity [θ].

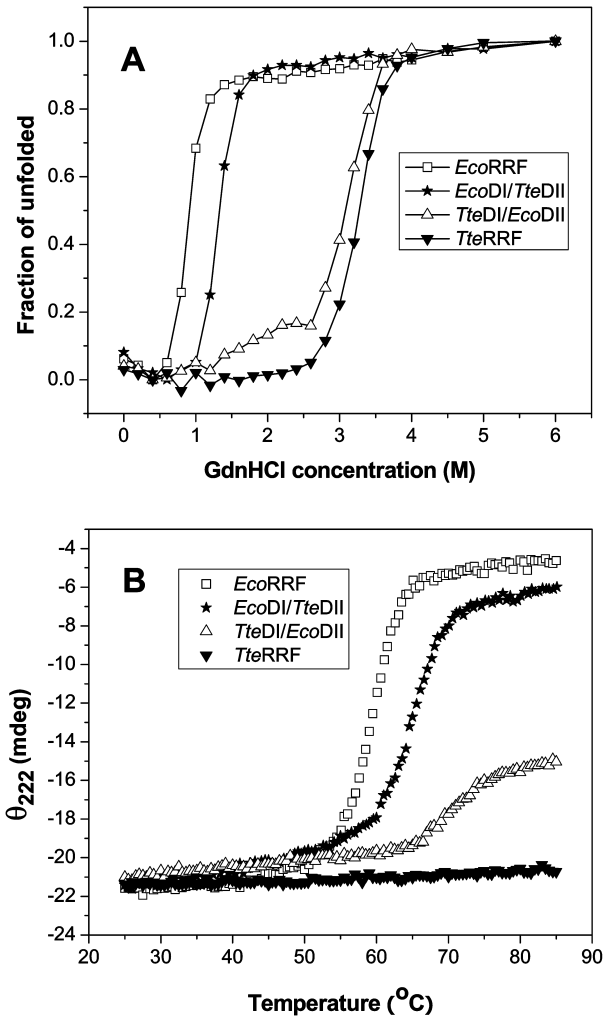

Fig. 8. **(A) GdnHCl-induced unfolding curves. (B) Heat-induced unfolding curves.** The experiments were performed as described in the text. These figures indicate that the *T. tengcongensis* domain I stabilizes the *Tte*DI/*Eco*DII RRF molecule, suggesting that domain I is mainly responsible for the stability of the RRF molecule.

chelating affinity chromatography (Fig. 2, lane 5). Eighty milligrams of purified His_6-tagged *Tte*RRF were obtained from one liter of bacterial culture under the shaking flask conditions. After cleavage of the purified His_6-tagged *Tte*RRF sample with thrombin, the cleaved mixture was subjected to the second metal chelating chromatography column to remove the fusion partner. About 50 mg of homogeneous protein (Fig. 2, lane 7) was obtained with a recovery of approximate 62.5%. Since a thrombin cleavage sequence is fused to the N-terminus of *Tte*RRF as shown in Fig. 1, there are four extra amino acid residues in the N-terminus of the RRF molecule.

Mass spectrographic analysis shows three peaks at *m*/*z* 21,488.22, 10,761.28, and 7,179.31, corresponding to single, double, and trinal protonated *Tte*RRF, respectively (Fig. 3). The molecular mass of *Tte*RRF obtained by mass spectrometry is consistent with the theoretical value calculated from amino acid composition of the protein (21,516.62). The results also indicate that thrombin cleavage under the above conditions is efficient.

There was antigenic cross-reactivity of *Tte*RRF with an antibody against *E. coli* RRF. As shown in Fig. 4, the purified *Tte*RRF cross-reacted with a polyclonal anti-*Eco*RRF antibody, although approximately 3-fold more *Tte*RRF was required to obtain an equivalent reaction with anti-*Eco*RRF than *E. coli* RRF.

To investigate whether *Tte*RRF is able to complement *E. coli* LJ14 (*frr*^{ts}), we monitored the growth of transformants harboring either vector alone (pQE-60) or the recombinants, pQE-*Eco*RRF and pQE-*Tte*RRF, which express *Eco*RRF and *Tte*RRF, respectively. As shown in Fig. 5, although all the transformants grew in liquid cultures at the permissive temperature (30°C), only the transformant harboring pQE-*Eco*RRF grew well at the non-permissive temperature (42°C), indicating that wild-type *Eco*RRF is able to complement the temperature-sensitive phenotype of *E. coli* LJ14 (*frr*^{ts}) efficiently. It is noteworthy that compared with pQE-60, slow growth of the transformant harboring pQE-*Tte*RRF was observed after prolonged incubation, suggesting that weak residual activity may remain in *Tte*RRF under heterologous conditions.

In this study, the primary and secondary structures of RRFs from *T. tengcongensis* and *E. coli* bacteria were compared. As shown in Fig. 6, the *T. tengcongensis* RRF protein contains 184 amino acid residues. The deduced amino acid sequence of *T. tengcongensis* RRF shows 51.4% identity and a 68.1% similarity to that of *E. coli* RRF. This high level of homology corresponds well to the high antigenic cross-reactivity of *Tte*RRF with the antibody against *E.coli* RRF.

Based on the X-ray structures of RRFs (*8*, *10*, *11–13*), Domain I of RRF consists of three long α-helices. This property makes RRF a suitable molecule for CD spectroscopic analysis. Far-UV CD spectroscopic analysis shows that the secondary CD profiles of *Tte*RRF, *Eco*RRF, and their chimeric proteins are very similar (Fig. 7), suggesting that the RRFs have the very similar secondary structures. Such high similarity in primary and secondary

structures implies that they have similar tertiary structures, although the three dimensional structure of *Tte*RRF is not yet available.

Characterization of Stability of Wild-Type RRFs and Their Chimeric RRFs Using GdnHCl and Heat Induced Denaturation—To test the changes in stability of the chimeric RRFs, and to find which domain is mainly responsible for maintaining the stability of RRF molecules, GdnHCl and heat induced denaturation of *Tte*RRF, *Eco*RRF, and their chimeric RRFs was measured by monitoring changes in the circular dichroism (CD) signal at 222 nm. Figure 8A shows the GdnHCl-induced unfolding of RRFs. It can be seen that the unfolding curve of *Eco*DI/*Tte*DII is close to that of *Eco*RRF, while the unfolding curve of *Tte*DI/*Eco*DII is close to that of *Tte*RRF. The heat induced denaturation of RRFs is shown in Fig. 8B. The thermostability of *Eco*DI/*Tte*DII is also close to that of *Eco*RRF, while *Tte*DI/*Eco*DII is close to that of *Tte*RRF. These results indicate that the *T. tengcongensis* domain I stabilizes the *Tte*DI/*Eco*DII RRF molecule, suggesting that domain I is mainly responsible for the stability of the RRF molecule. This will help in further studies of the molecular mechanisms of protein thermostability.

We thank Professor A. Kaji, Department of Microbiology, School of Medicine, University of Pennsylvania, for providing *E. coli* LJ14 strain. This work was supported by grants (Nos. G1999075608 and 30170210) from the China Committee for Science and Technology.

REFERENCES

1. Jaenicke, R., Schurig, H., Beaucamp, N., and Ostendorp, R. (1996) Structure and stability of hyperstable proteins: Glycolytic enzymes from hyperthermophilic bacterium *Thermotoga maritima*. *Adv. Protein Chem.* **48**, 181–269
2. Janosi, L., Hara, H., Zhang, S., and Kaji, A. (1996) Ribosome recycling by ribosome recycling factor (RRF)—an important but overlooked step of protein biosynthesis. *Adv. Biophys.* **32**, 121–201
3. Kaji, A., Teyssier, E., and Hirokawa, G. (1998) Disassembly of the post-termination complex and reduction of translational error by ribosome recycling factor (RRF)—a possible new target for antibacterial agents. *Biochem. Biophys. Res. Commun.* **250**, 1–4
4. Janosi, L., Ricker, R., and Kaji, A. (1996b) Dual functions of ribosome recycling factor in protein biosynthesis: disassembling the termination complex and preventing translational errors. *Biochimie* **78**, 959–969
5. Kaji, A., Kiel, M.C., Hirokawa, G., Muto, A., Inokuchi, Y., and Kaji, H. (2001) The fourth step of protein synthesis: disassembly of the post-termination complex is catalyzed by elongation factor G and ribosome recycling factor, RRF, a near perfect mimic of t RNA. *Cold Spring Harb. Symp. Quant. Biol.* **66**, 515–529
6. Nakamura, Y., Ito, K., and Isaksson, L.A. (1996) Emerging understanding of translation termination. *Cell* **87**, 147–150
7. Pavlov, M.Y., Freistroffer, D., MacDougall, J., Buckingham, R.H., and Ehrenberg, M. (1997) Fast recycling of *Escherichia coli* ribosomes requires both ribosome recycling factor (RRF) and release factor RF3. *EMBO J.* **16**, 4134–4141
8. Toyoda, T., Tin, O.F., Ito, K., Fujiwara, T., Kumasaka, T., Yamamoto, M., Garber, M.B., and Nakamura, Y. (2000) Crystal structure combined with genetic analysis of the *Thermus thermophilus* ribosome recycling factor shows that a flexible hinge may act as a functional switch. *RNA* **6**, 1432–1444
9. Nakano, H., Yoshida, T., Uchiyama, S., Kawachi, M., Matsuo, H., Kato, T., Ohshima, A., Yamaichi, Y., Honda, T., Kato, H., Yamagata, Y., Ohkubo, T., and Kobayashi, Y. (2003) Structure and binding mode of a ribosome recycling factor (RRF) from Mesophilic bacterium. *J. Biol. Chem.* **278**, 3427–3436
10. Selmer, M., Al-Karadaghi, S., Hirokawa, G., Kaji, A., and Liljas, A. (1999) Crystal structure of *Thermotoga martima* ribosome recycling factor: A tRNA mimic. *Science* **286**, 2349–2352
11. Kim, K.K., Min, K., and Suh, S.W. (2000) Crystal structure of the ribosome recycling factor from *Escherichia coli*. *EMBO J.* **19**, 2362–2370
12. Nakano, H., Uchiyama, S., Yoshida, T., Ohkubo, T., Kato, H., Yamagata, Y., and Kobayashi, Y. (2002) Crystallization and preliminary X-ray crystallographic studies on of a mutant of ribosome recycling factor from *Escherichia coli*, Arg132Gly. *Acta crystal. D* **58**, 124–126
13. Saikrishnan, K., Kalapala, S.K., Varshney, U., and Vijayan, M. (2005) X-ray structural studies of Mycobacterium tuberculosis RRF and a comparative study of RRFs of known structure. *Mol. Plastic. Biol. Implicat.* **345**, 29–38
14. Bao, Q., Tian, Y., Li, W., Xu, Z., Xuan, Z., Hu, S., Dong, W., Yang, J., Chen, Y., Xue, Y., Xu, Y., Lai, X., Huang, L., Dong, X., Ma, Y., Ling, L., Tan, H., Chen, R., Wang, J., Yu, J., and Yang, H. (2002) A complete sequence of the *Thermoanaerobacter tengcongensis* genome. *Genome Res.* **12**, 689–700
15. Janosi, L., Mottagui-Tabar, S., Isaksson, L.A., Sekine, Y., Ohtsubo, E., Zhang, S., Goon, S., Nelken, S., Shuda, M., and Kaji, A. (1998) Evidence for *in vivo* ribosome recycling, the fourth step in protein biosynthesis. *EMBO J.* **17**, 1141–1151
16. Zhang, X.L., Guo, P., and Jing, G.Z. (2003) A vector with the downstream box of the initiation codon can highly enhance protein expression in *Escherichia coli*. *Biotech. Lett.* **25**, 755–760
17. Etchegargy, J.P. and Inouye, M. (1999) Tanslation enhancement by an element downstream of the initiation codon in *Escherichia coli*. *J. Biol. Chem.* **274**, 10079–10085
18. Horton, R.M., Cai, Z., Ho, S.N., and Pease, L.R. (1990) Gene splicing by overlap extension: Tailor-made genes using the polymerase chain reaction. *Biotechniques* **8**, 528–535
19. Blackshear, P.J. (1984) System for polyacrylamide gel electrophoresis. *Methods Enzymol.* **68**, 237–255
20. Zhou, B. and Jing, G.Z. (1999) Determination of protein extinction coefficients by alkaline hydrolysis. *Prog. Biochem. Biophys.* **26**, 384–387
21. Harlow, E. and Lane, D. (1988) *Antibodies: A Laboratory Manual*, Cold Spring Harbor Laboratory Press, Cold Spring Harbor, NY
22. Trojanowski, J.Q., Obrocka, M.A., and Lee, V.M. (1983) A comparison of eight different chromogen protocols for the demonstration of immunoreactive neurofilaments or glial filaments in rat cerebellum using the peroxidase-antiperoxidase method and monoclonal antibodies. *J. Histochem. Cytochem.* **31**, 1217–1223